

Supporting Information for *Chemical Science*

Pb(II) Metal-Organic Nanotubes Based on Cyclodextrins: Biphasic Synthesis, Structures and Properties

Yanhui Wei,^a Di Sun,^a Daqiang Yuan,^b Yongjun Liu,^a Yi Zhao,^a Xiyu Li,^a Suna Wang,^c
Jianmin Dou,^c Xingpo Wang,^a Liangliang Zhang,^a Aiyu Hao,^a Daofeng Sun^{*ab}

Key Lab for Colloid and Interface Chemistry of Education Ministry, School of Chemistry and
Chemical Engineering, Shandong University, Jinan 250100, People's Republic of China

State Key Laboratory of Structural Chemistry, Fujian Institute of Research on the Structure of Matter,
Chinese Academy of Sciences, Fujian, Fuzhou, 350002, People's Republic of China

Department of Chemistry, Liaocheng University, Liaocheng, 252059, P. R. China

E-mail: dfsun@sdu.edu.cn.

General Information. Commercially available reagents were used as received without further purification. Both cyclodextrins were further purified by recrystallization from water. ¹H NMR spectra were recorded on a Bruker AVANCE-400 NMR Spectrometer. Elemental analysis was carried out on a CE instruments EA 1110 elemental analyzer. Photoluminescence spectra were performed on a F-280 Fluorescence Spectrophotometer. X-ray powder diffractions were measured on a Bruker AXS D8 Advance. Thermogravimetric analysis (TGA) was carried out in a static N₂ with a heating rate of 10 °C/min. CD spectra were recorded on a JASCO J-810. SEM was obtained on a JEOL JSM-6700F. The solid-state diffuse-reflectance UV/vis spectra for powder samples were performed on a 2800UV/VIS spectrometer equipped with an integrating sphere by using BaSO₄ as a white standard.

Table S1. Crystal Data Collection and Structure Refinement for **CD-MONT-2** and **CD-MONT-3**.

	CD-MONT-2	CD-MONT-3
empirical formula	C _{101.5} H _{146.5} O ₉₆ Pb ₁₄	C ₉₆ H ₁₂₈ O ₈₉ Pb ₁₆
formula weight	5803.35	6021.02
temp (K)	200	200
crystal system	orthorhombic	monoclinic
space group	<i>P</i> 2 ₁ 2 ₁ 2 ₁	<i>P</i> 2 ₁
<i>a</i> (Å)	15.6077(13)	20.126(3)
<i>b</i> (Å)	24.196(2)	18.866(3)
<i>c</i> (Å)	38.766(3)	22.188(4)
α (deg)	90	90
β (deg)	90	94.783(2)
γ (deg)	90	90
<i>V</i> (Å ³)	14640(2)	8395(2)
<i>Z</i>	4	2
ρ calc (g/cm ³)	2.633	2.382
<i>F</i> (000)	10686	5456
data/restraints/params	24936/0/1879	28929/15/1790
GOF on <i>F</i> ²	1.004	1.039
final <i>R</i> indices [<i>I</i> > 2 σ (<i>I</i>)]	<i>R</i> ₁ = 0.0285, <i>wR</i> ₂ = 0.0609	<i>R</i> ₁ = 0.0588, <i>wR</i> ₂ = 0.1516

Adsorption of I₂ experiment:

In the adsorption experimental process, the crystals of **CD-MONT-2** and **CD-MONT-3** were heated to 160 °C for half an hours to release all the solvents in the cavities, then immersed in toluene solution of I₂ (0.005 M/L, 2 mL) in a sealed vial at 15 °C. The colors of the crystals changed from colorless to brown and yellow for **CD-MONT-2** and **CD-MONT-3**, respectively, and the color of the solution changed from deep pink to almost colorless after 78 hours.

Photoluminescence measurement:

All the solid-state luminescent measurement were performed on a F-280 Fluorescence Spectrophotometer. All instrument paraments including excitation/emmission slit and scanning speed were fixed for all measurement. In order to

ensure the luminescence intensity differences among the samples reliable, we divided the sample into three parts in same weight (30 mg) for thermal activation, and I₂ adsorption. The samples were squashed into three plates in the same thickness and size for the photoluminescence measurement.

The as-synthesized samples were heated to 120 °C for half an hour to release all the solvents, then were squashed into plates for luminescence measurement. The activated samples were immersed in toluene solution of I₂ (0.005 M, 0.5 mL) for 78 hours. After washed with fresh toluene for several times, the I₂-loaded samples were squashed into plates for further luminescence measurement.

Calculation method:

To understand the different behaviors of α -, β -, γ -Cyclodextrins, the first principle calculations were performed on the complexes of α -, β -, γ -Cyclodextrins that cooperated with Pb^{2+} by using hybrid density functional theory method, in which the Beck three-parameter nonlocal exchange functional with the correction functional of Lee-Yang-Parr (B3LYP) was used. For the complexes of β -, γ -Cyclodextrins, the initial geometries were derived from the crystal structures, and that of α -Cyclodextrin was obtained from β -Cyclodextrin by cutting one pair of glucopyranose rings.

Firstly, the complexes of α, β, γ -Cyclodextrins were fully optimized (See Fig. S15). The effective-core-potential LANL2DZ basis set was used for Pb atom, and 3-21G basis set was used for C, H and O atoms. For comparison, we also optimized a model compound which contains three Pb^{2+} and eight cooperated CH_3O^- group, and calculated the single point energies of three segments that truncated from α -, β -, γ -Cyclodextrins complexes (See Fig. S17) by using 6-31G(d, p) basis set for C, H and O atoms. The calculation results reveal that the structural parameters of glucopyranose rings show neglectable differences, but those of parameters related to Pb atom display some changes. The key parameters and relative energies of the three segments are listed in Table S2. For clarity, in the calculation part, we name the complex based on α -Cyclodextrin as **CD-MONT-1**.

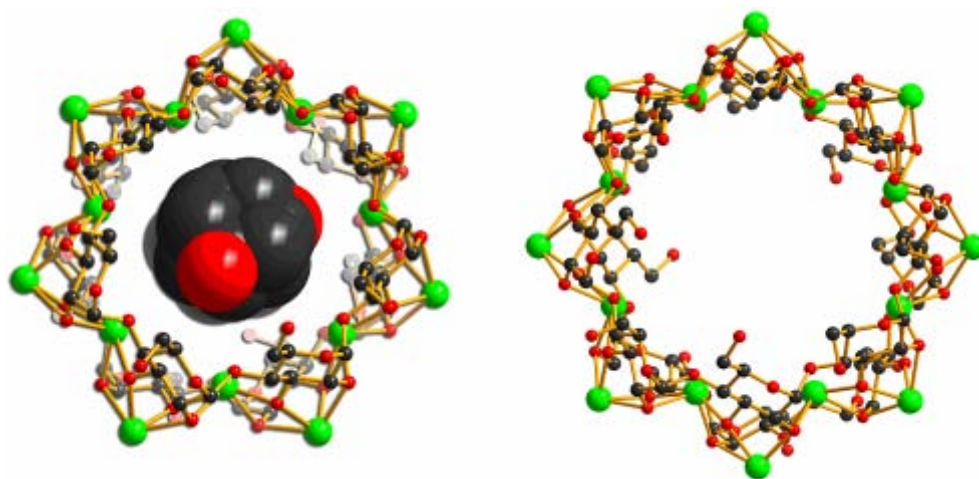


Figure S1. The nanotubes of **CD-MONT-2** (left) and **CD-MONT-3** (right) with and without guest solvents, respectively.

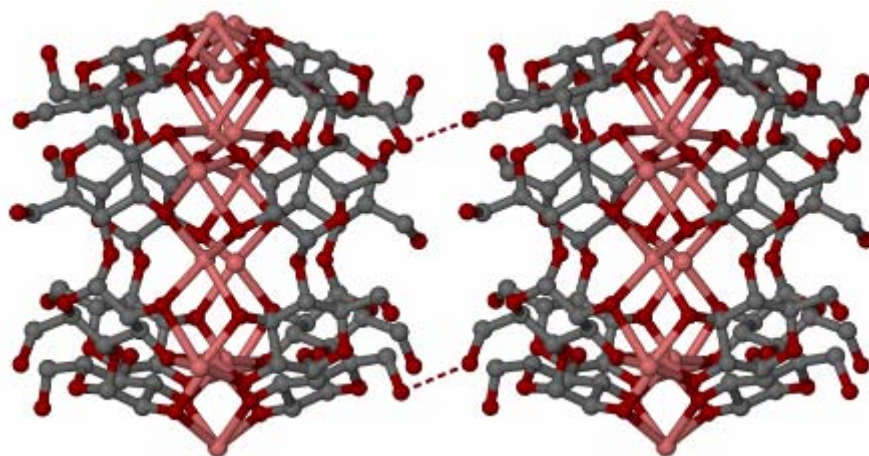


Figure S2. The hydrogen bonding interaction between two nanotubes in **CD-MONT-2**.

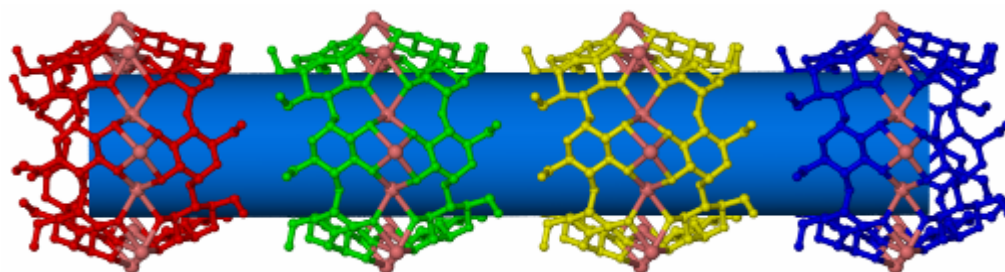


Figure S3. The 1D supramolecular nanotube in **CD-MONT-2** formed by the hydrogen bonding interactions.

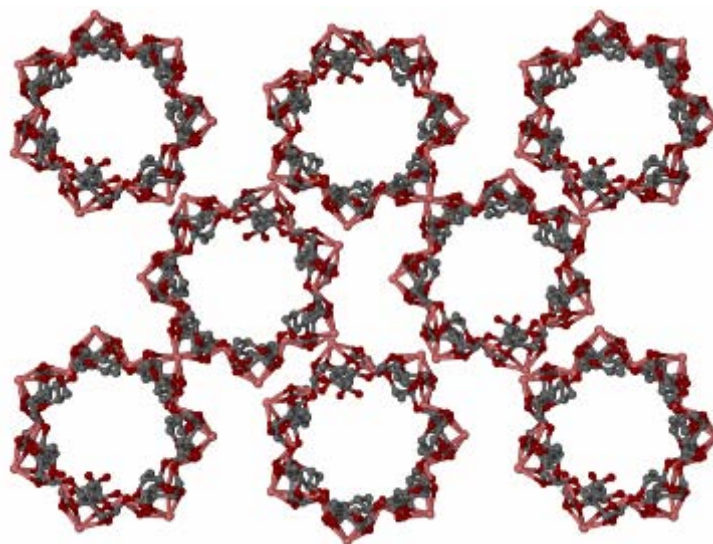


Figure S4. The 3D supramolecular architecture in **CD-MONT-2**, showing the 1D channels.

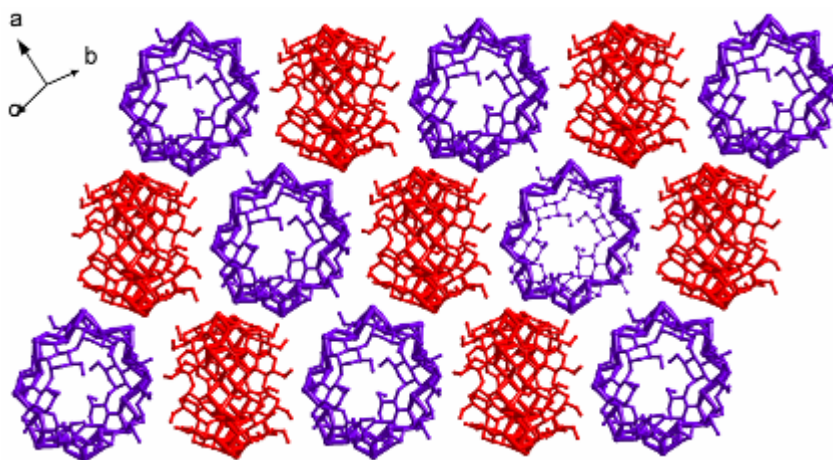


Figure S5. The arrangement of CD-MONT-3 along two different directions.



Figure S6. Photographs of the as-synthesized crystals of **CD-MONT-2** (left) and **CD-MONT-3** (right).

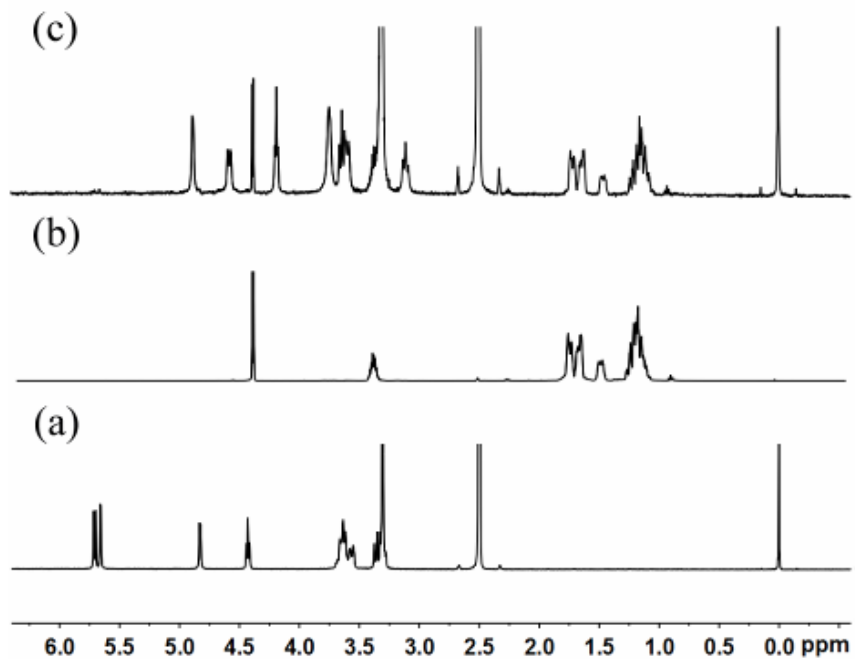


Figure S7. The NMR spectra of (a) β -cyclodextrin; (b) cyclohexanol molecules and (c) CD-MONT-2 in d_6 -DMSO.

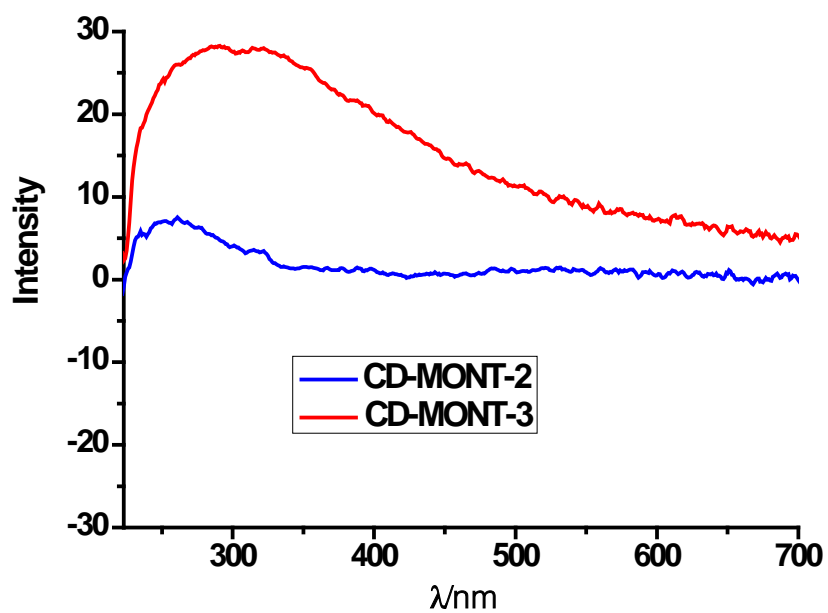


Figure S8. The CD spectra of CD-MONT-2 and CD-MONT-3.

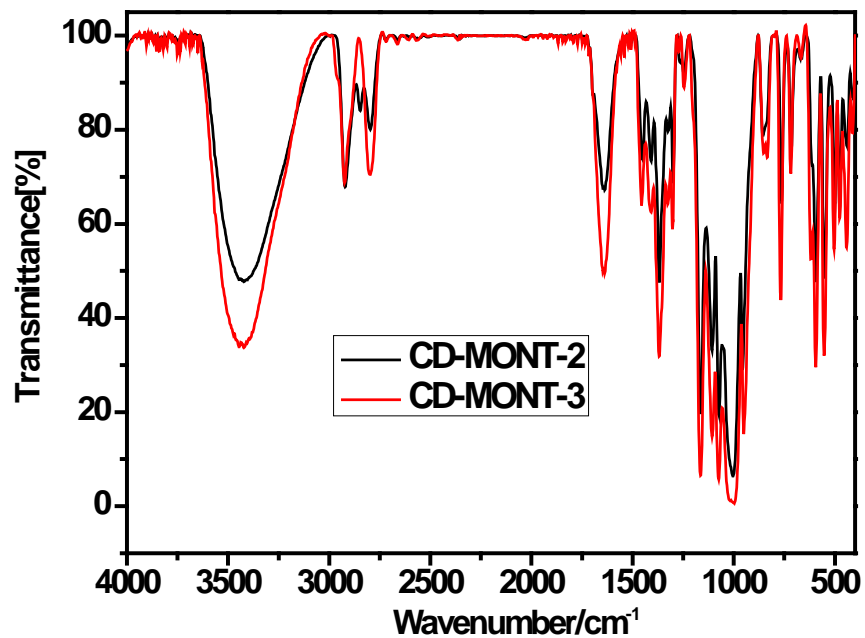


Figure S9. The IR spectra of CD-MONT-2 and CD-MONT-3.

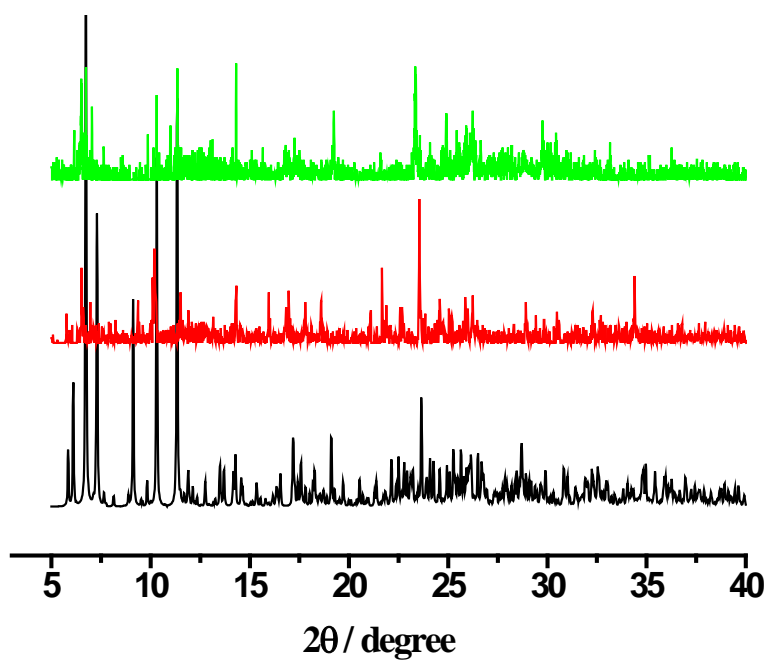


Figure S10. X-ray powder diffraction patterns (Cu K α_1) of CD-MONT-2, black, simulated based on crystal data; red, asynthesized; green, after heated to 120 °C for half an hour.

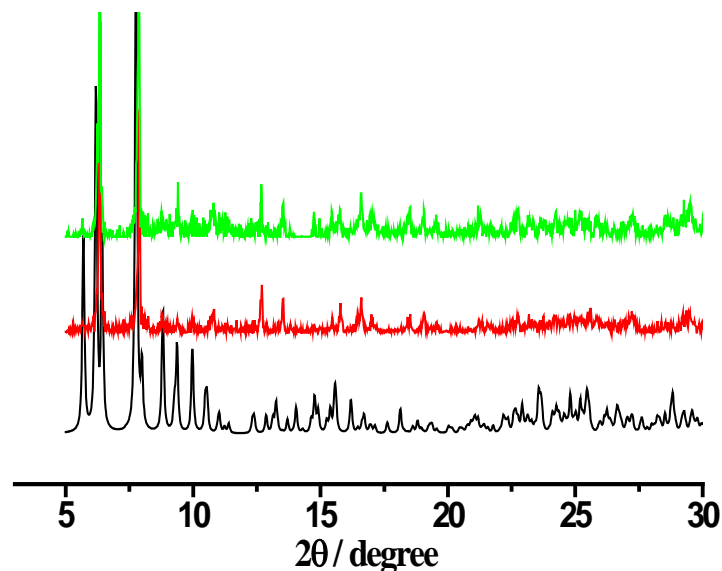


Figure S11. X-ray powder diffraction patterns ($\text{Cu K}\alpha_1$) of **CD-MONT-3**, black, simulated based on crystal data; red, as-synthesized; green, after heated to 120 °C for half an hour.

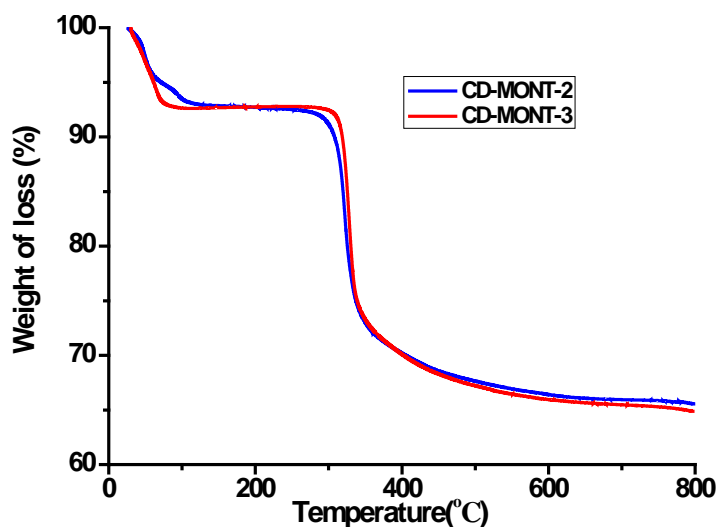


Figure S12. The TGA for **CD-MONT-2** and **CD-MONT-3**. Based on the TGA, these two MONTs possess similar thermal behaviors. For **CD-MONT-2**, the guest solvents were completely removed from 50 to 120 °C, and the framework can be stable up to 270 °C. For **CD-MONT-3**, the guest solvents were completely removed from 50 to 85 °C, and the framework can be stable up to 300 °C. Both materials were finally decomposed to PbO powders after 800 °C.

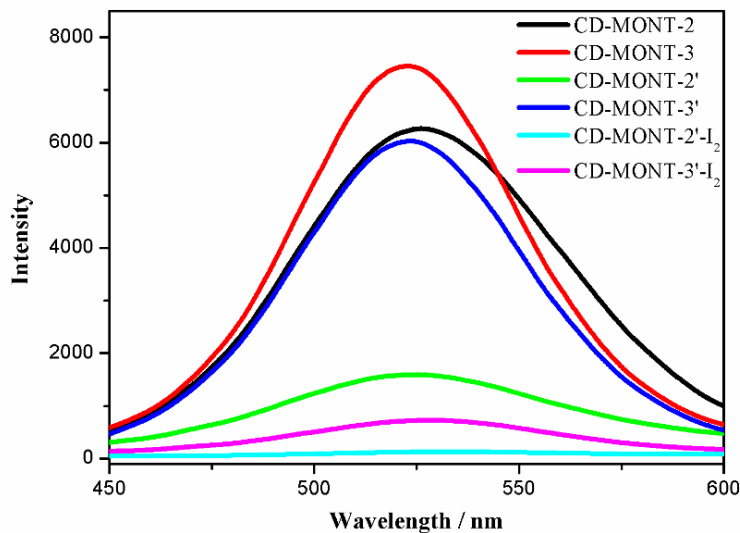


Figure S13. Comparison emission behaviors among CD-MONT, CD-MONT', and CD-MONT'-I₂.

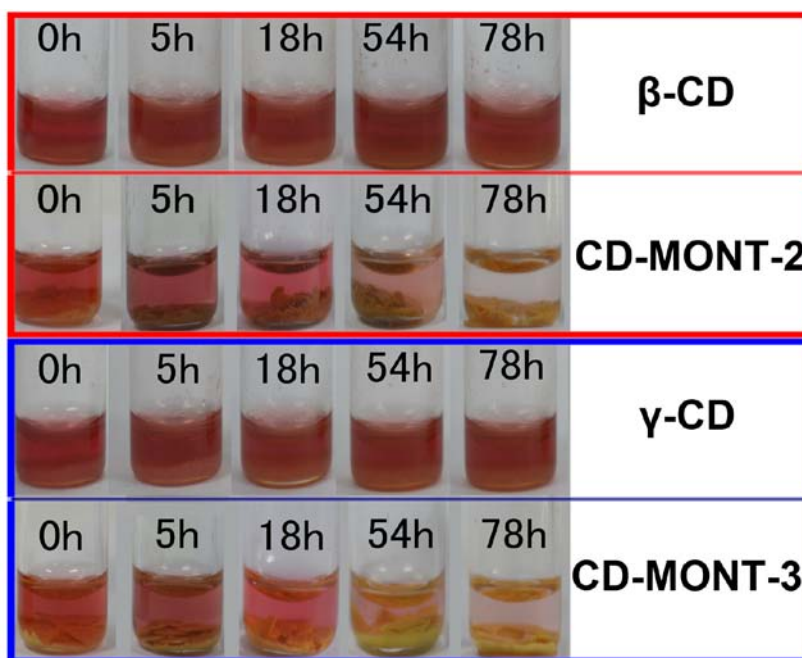


Figure S14. Comparisons of adsorption of iodine molecules between β -CD, γ -CD molecules and CD-MONT-2, CD-MONT-3, respectively, under the same condition. The experiment that the iodine solutions are exposed only to bulk cyclodextrin powders has been carried out. These additional experiments indicate that the iodine molecules are adsorbed in the cavities of the materials.

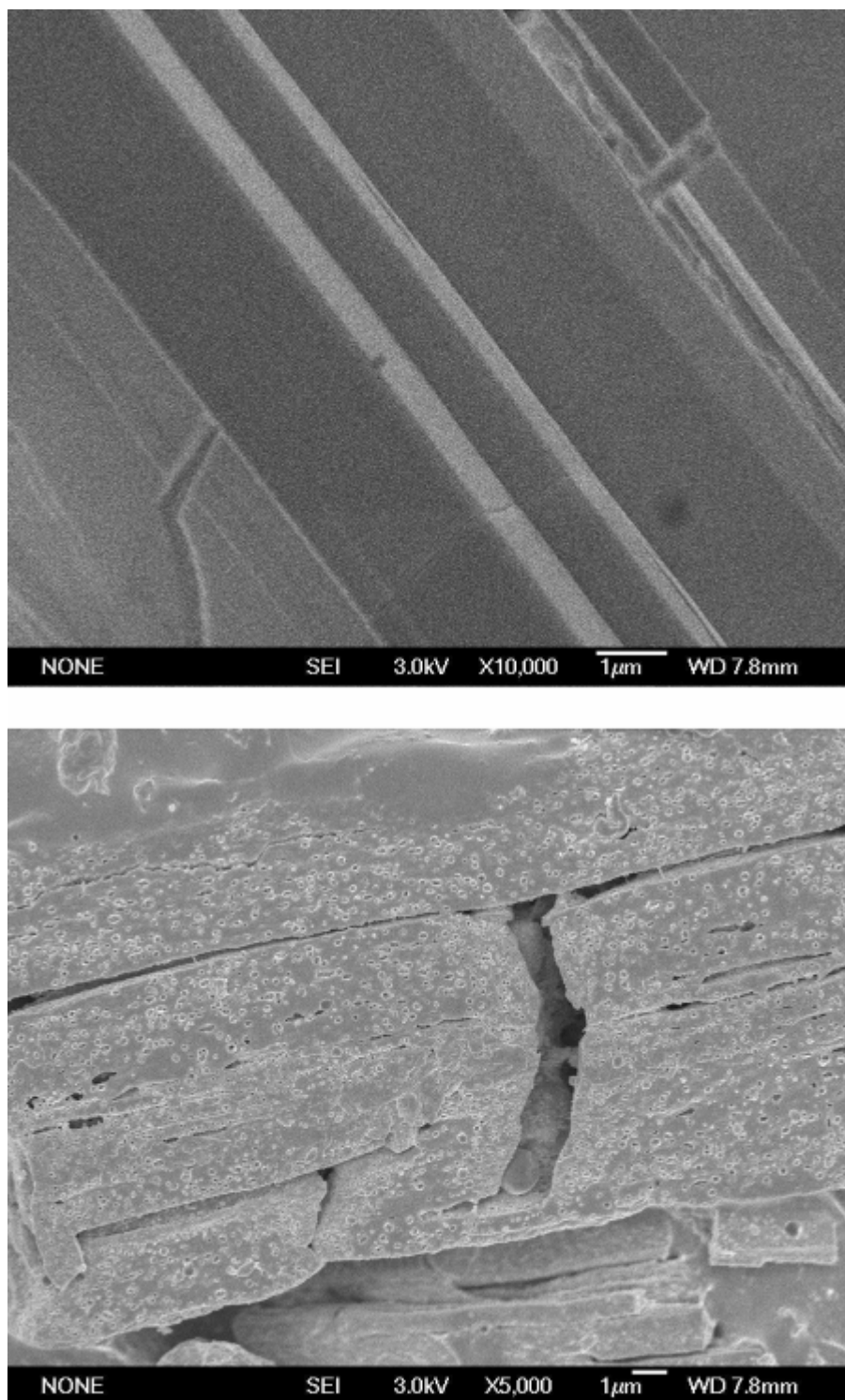


Figure S15. The SEM photographs of **CD-MONT-2** before (top) and after (bottom) heated to 800 °C for 1h.

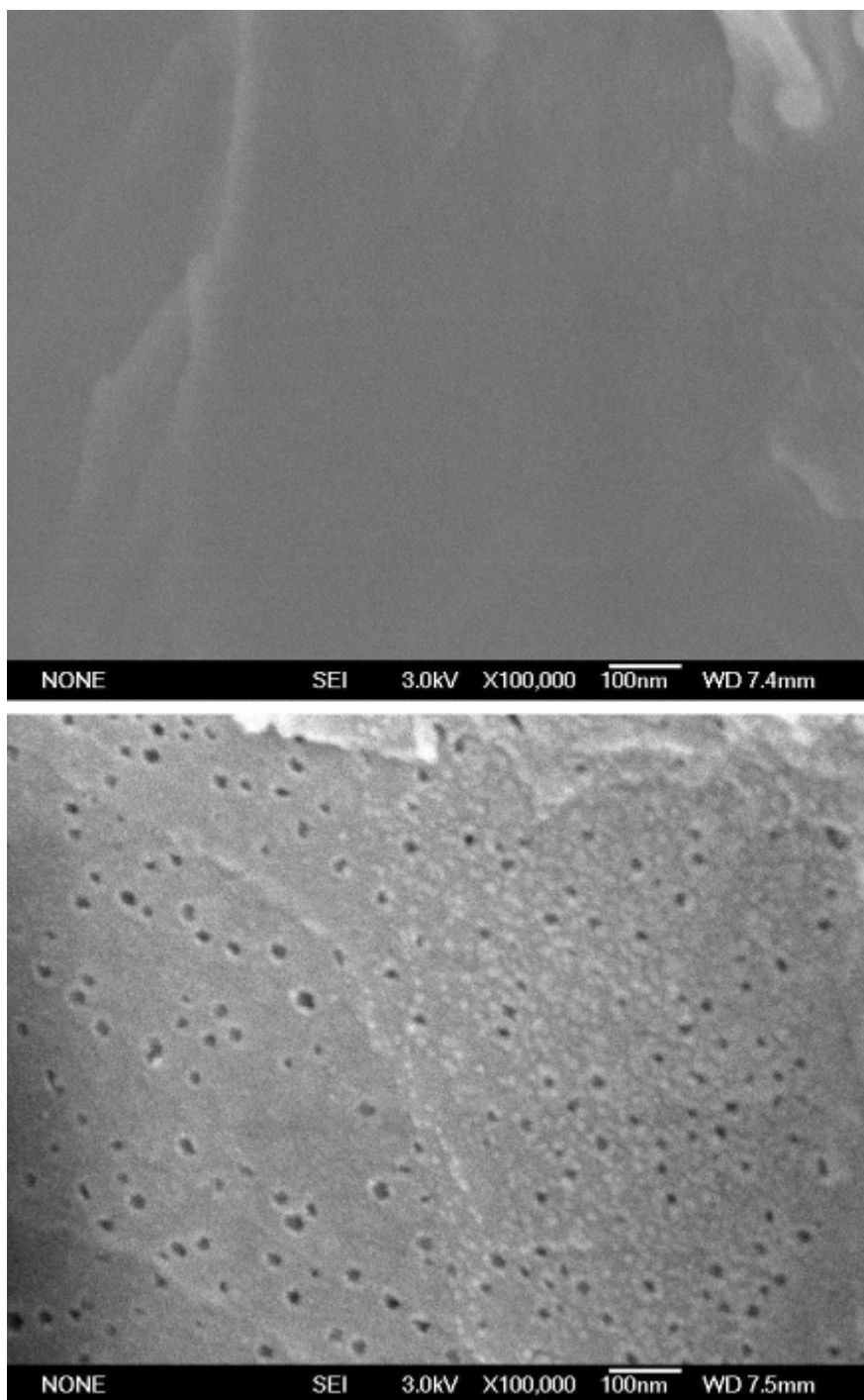


Figure S16. The SEM photographs of **CD-MONT-3** before (top) and after (bottom) heated to 800 °C for 1h.

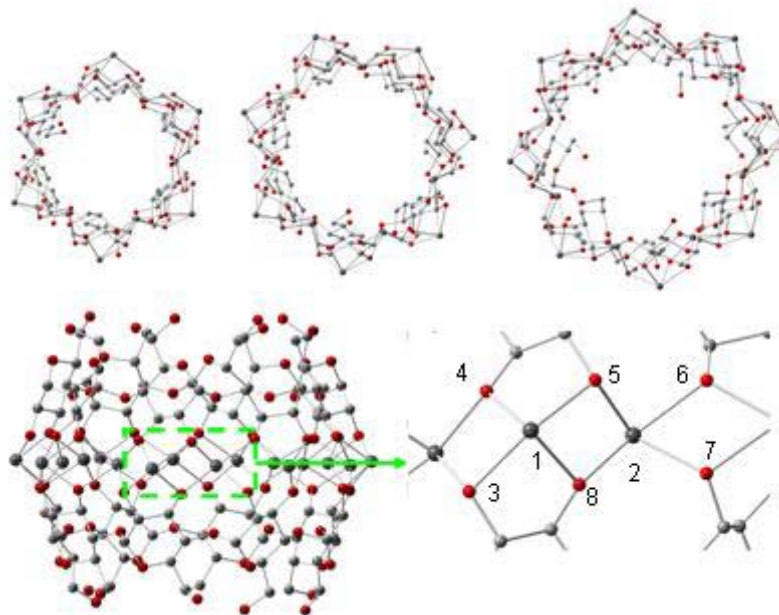


Figure S17. The optimized structures of complexes of **CD-MONT-1-3**, and labels of atoms.

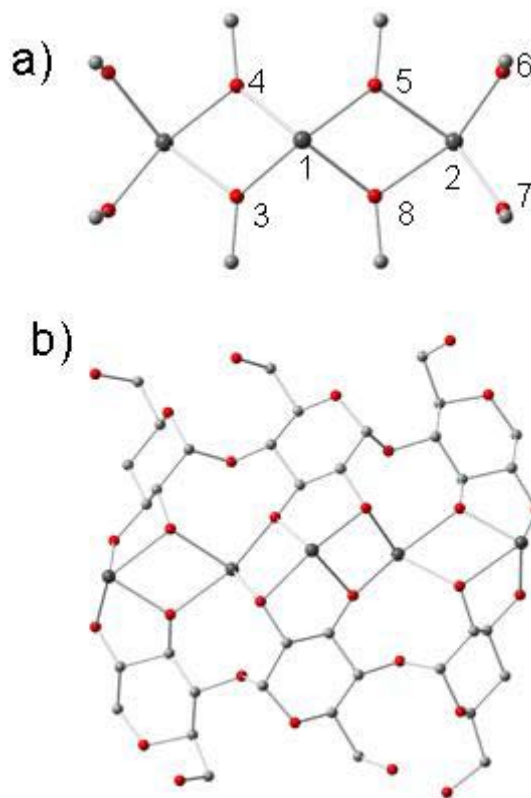


Figure S18. a) The optimized structure of model compound; b) The structure of a segment used for single point energy calculation.

Table S2. Key structural parameters and relative energies of three segments.

	CD-MONT-1	CD-MONT-2	CD-MONT-3	Model compound
Angle (O ₃ -Pb ₁ -O ₅) ^a	126.5	127.0	127.3	125.4
Angle (O ₄ -Pb ₁ -O ₈)	99.5	98.7	98.6	125.4
Angle (O ₈ -Pb ₂ -O ₆)	147.4	145.5	143.7	126.7
Angle (O ₅ -Pb ₂ -O ₇)	111.7	109.9	109.3	126.7
Dihedral angel (Pb ₁ -O ₅ -Pb ₂ -O ₈)	-15.6	-13.1	-11.0	-4.1
Relative energies of segments (Kcal/mol)	97.3	17.2	0.0	

^aAll the angles and dihedral angels are averaged data and in degree.

Table S2 shows that, in the model compound the angles of O₃-Pb₁-O₅ and O₈-Pb₂-O₆ are almost equal (125.4° vs 126.7°), and the dihedral angel of Pb₁-O₅-Pb₂-O₈ is only -4.1°. But in **CD-MONT-1-3**, all the angles were distorted. For example, the dihedral angel of Pb₁-O₅-Pb₂-O₈ in **CD-MONT-1** is as large as -15.6° duo to the distortion. As a result, the relative energy of the segment in **CD-MONT-1** and **CD-MONT-2** are 97.3 and 17.2 kcal/mol higher that that of **CD-MONT-3**, indicating that the formation of **CD-MONT-1** is difficult, compared to the formation **CD-MONT-2** and **CD-MONT-3**.

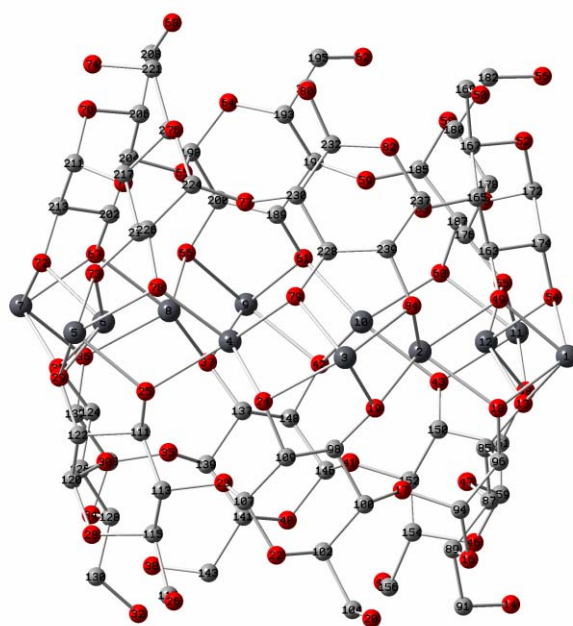


Figure S19. The optimized structure of **CD-MONT-1**.

Table S3. The angle of O-Pb-O and dihedral angel (Pb-O-Pb-O) in **CD-MONT-1**.

	Angle (O-Pb-O) (Pb: outside)		Angle(O-Pb-O) (Pb: inside)		dihedral angel (Pb-O-Pb-O)		
1	126.5	99.7	2	111.5	147.7	1,2	-15.9
						2,3	-15.4
3	126.5	99.4	4	111.2	147.1	3,4	-16.5
						4,5	-14.6
5	126.8	99.8	6	112.2	147.5	5,6	-15.2
						6,7	-15.8
7	126.2	99.5	8	112.5	147.5	7,8	-16.9
						8,9	-14.9
9	126.6	99.8	10	110.5	147.2	9,10	-15.7
						10,11	-15.4
11	126.6	98.6	12	112.5	147.5	11,12	-15.7
Average	126.5	99.5		111.7	147.4		-15.6

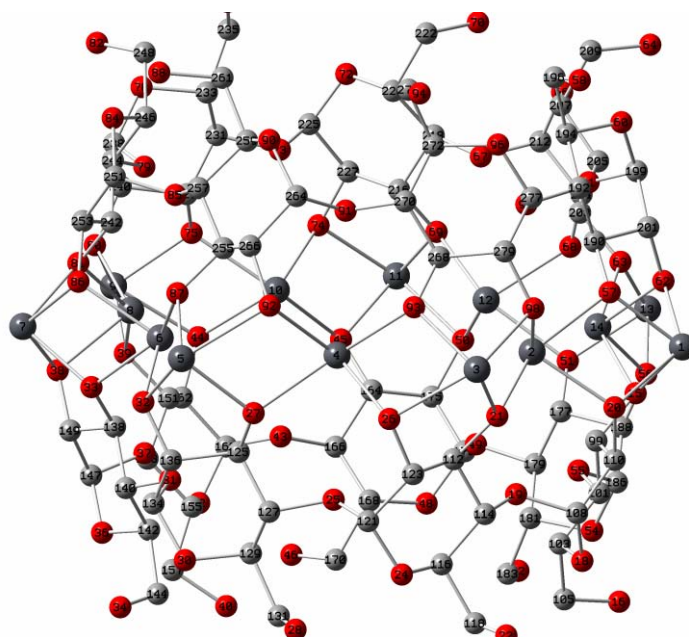


Figure S20. The optimized structure of **CD-MONT-2**.

Table S4. The angle of O-Pb-O and dihedral angel (Pb-O-Pb-O) in **CD-MONT-2**.

	Angle(O-Pb-O) (Pb: outside)		Angle(O-Pb-O) (Pb: inside)		dihedral angel (Pb-O-Pb-O)		
1	127.4	99.8	2	110.0	145.7	1,2	-13.0
						2,3	-13.2
3	127.0	97.4	4	110.0	145.7	3,4	-14.3
						4,5	-12.5
5	126.9	99.1	6	108.9	145.5	5,6	-12.7
						6,7	-11.9
7	127.3	98.7	8	110.9	145.2	7,8	-12.9
						8,9	-13.7
9	126.7	98.5	10	110.9	145.4	9,10	-14.4
						10,11	-12.2
11	127.1	99.2	12	108.3	145.7	11,12	-12.8
						12,13	-13.2
13	126.9	98.2	14	110.4	145.1	13,14	-12.9
Average	127.0	98.7		109.9	145.5		-13.1

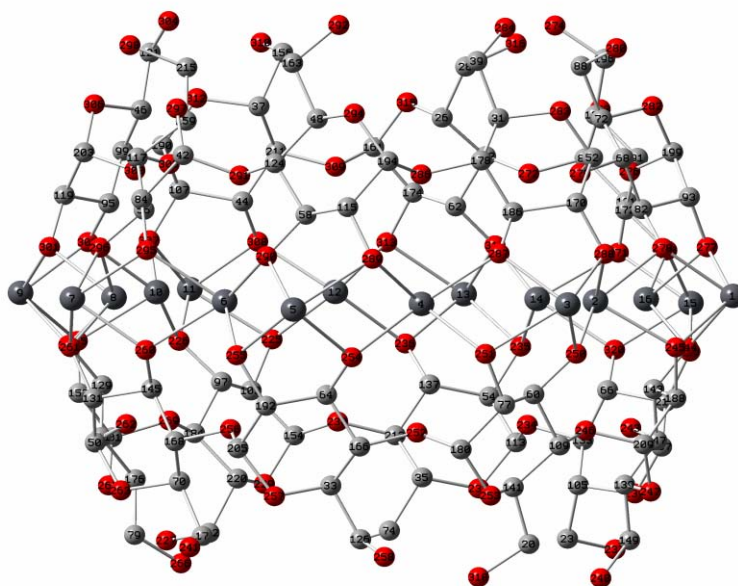


Figure S21. The optimized structure of **CD-MONT-3**.

Table S5. The angle of O-Pb-O and dihedral angel (Pb-O-Pb-O) in **CD-MONT-3**.

	Angle(O-Pb-O) (Pb: outside)		Angle(O-Pb-O) (Pb: inside)		dihedral angel (Pb-O-Pb-O)		
1	127.8	98.4	2	107.6	144.1	1,2	-11.7
						2,3	-11.2
3	126.1	99.8	4	107.6	144.2	3,4	-11.9
						4,5	-11.5
5	127.5	98.1	6	111.0	142.5	5,6	-11.2
						6,7	-9.0
7	128.3	98.7	8	108.7	143.6	7,8	-10.0
						8,9	-11.7
9	126.4	99.0	10	110.5	144.8	9,10	-13.2
						10,11	-11.0
11	127.7	97.3	12	108.2	143.9	11,12	-11.0
						12,13	-8.9
13	127.7	99.0	14	108.1	144.5	13,14	-10.7
						14,15	-10.2
15	127.1	98.2	16	112.9	142.0	15,16	-12.5
Average	127.3	98.6		109.3	143.7		-11.0